Vol. 10(1), pp. 1-16, January-June 2021
DOI: 10.5897/JBD2021.0056
Article Number: 2F8A9EB66877
ISSN 2141-2197

http://www.academicjournals.org/JBD

ACADEMIC JOURNALS
expand your knowledge

Journal of Brewing and Distilling

Full Length Research Paper

Malt roasting quality control by mid-infrared spectroscopy

Deborah Herdt[1*], Tobias Teumer[1], Sindhu Nair Balan[1], Nur Adibah Kamarulzman[1], Thomas Kunz[2], Sarah Kühnemuth[2] Frank-Jürgen Methner[2] and Matthias Rädle[1]

[1]Center for Mass Spectrometry and Optical Spectroscopy, Mannheim University of Applied Sciences, Mannheim, Germany.
[2]Institute of Food Technology and Food Chemistry, Technische Universität Berlin, Berlin, Germany.

Received 20 January, 2021; Accepted 22 April, 2021

In the presented investigation, the chemical composition of malt during roasting is estimated using diffuse reflectance mid-infrared fourier transform (DRIFT-MIR) spectroscopy and multiple linear regressions. Accordingly, the corresponding test setup is presented and evaluated. A total number of sixty-five stop roasting, having temperature range from 140 to 220ºC, and one unroasted sample of 1500 g Avalon malt are performed in an eddy current roaster. Roasted and unroasted malt samples are milled and then analysed. Additionally, analytical standard reference methods are performed for colour, spectral tristimulus L*a*b* - values, colour difference (ΔE), iron-content, quantitative radical generation and the formation of specific intermediates, such as 5-(hydroxymethyl) furfural (HMF) as well as 3-deoxy-hexosulose (3-DH) and end products of Maillard reaction on all sixty-six samples. Multiple linear regression models were used to predict analysed references based on mid-infrared data, modified with spectral pre-processing for better prediction performance. The obtained results indicate that DRIFT-MIR spectrometry, combined with pre-processing and selection of evaluated wave number areas, is a useful analytical tool for the measurement of quality attributes of malt and therefore, shows potential for application in quality and process control.

Key words: Malt roasting, mid-infrared, optical spectroscopy, process control, EBC, L*a*b*, ΔE, quality control.

INTRODUCTION

Roasting of malt or barley is a crucial step of roast-, caramel- and malt production which defines physical, structural and chemical properties (Yahya et al., 2014). Several compounds like polyphenols, protein fraction, amino acids, etc. originating from barley, and Maillard reaction products (MRPs) (Carvalho et al., 2014), generated during malting, and are found in malt (Goupy et al., 1999; Shahidi and Ambigaipalan, 2015; Woffenden et al., 2001; Wunderlich et al., 2013). Chemical composition of ingredients as well as the physical properties of malt e.g. colour or flavour are altered through roasting processes (Coghe et al., 2006; Martins et al., 2000; Mohsin et al., 2018). The on-going automation in food industry and rising requirements on

*Corresponding author. E-mail: d.herdt@hs-mannheim.de.

quality control demand real time online analytic techniques. Near infrared (NIR) spectroscopy has been used in many studies before to monitor the quality of protein content in barley and malt (Fox et al., 2002; Ratcliffe and Panozzo, 1999; Sá and Palmer, 2006; Schmidt et al., 2009) as well as physicochemical changes (Contreras-Jiménez et al., 2019).

A study by Kljusurić et al. investigated the determination of the optimal process conditions for barley milk by combining NIR spectroscopy with measuring particle size and conductivity of samples (Gajdoš Kljusurić et al., 2015). Moreover, barley analysis by NIR (Czuchajowska et al., 1992) and mid infrared (MIR) spectroscopy (Cozzolino et al., 2013; Cozzolino et al., 2014) has shown to be useful for prediction models of malt quality. The possibility to control malt roasting and therefore, to define a stop criterion for targeted roast malt colour, is a challenging topic (Bamforth, 2017).

The malt colour shift is specified by MEBAK (Methodensammlung der Mitteleuropäischen Brautechnischen Analysenkommission) (Jacob, 2016) as EBC (European Brewery Convention) value (Miedaner, 2002). EBC value estimation is a method to determine the colour of wort and beer under defined conditions. Beer is decarboxylated; turbid samples are taken and afterwards; membrane is filtered. The EBC value is then determined by simply comparing the beer colour with a standardized scale. A previously established method, the Lovibond common technique, a visual method which is revised (Bishop 1950, 1966; Sharpe et al., 1992; Smedley, 1992). One possible error source of this method is that subjective perception of each person varies and, consequently, shows the differences in the colour values.

An alternative of the above-mentioned technique is spectrophotometric method in which subjective influences of the human eye are eliminated. This method is used in this work as a reference. The measurement is performed in a 10 mm cuvette at a wavelength of 430 nm (Farber and Barth, 2019; Miedaner, 2002). The sample is diluted to access absorbance in the linear range of the visible spectrophotometer. However, the accuracy of this method is quite low (Hans, 2009).

In addition to the EBC values, there is also the SRM (Standard Reference Method) (Miedaner, 2002) value, which can be converted into the EBC value using a factor of 1.97. Another measuring concept is considering different colours of varieties of beer, a method put forth by the Commission Internationale d'Eclairage. This technique comprises L*, a* and b* values and is called tristimulus CIE Lab colour (Bamforth, 2009; Mallet, 2014). This is used as a reference method to determine the change of colour during the roasting process. This study is conducted to identify optimal roasting temperatures with reference methods. The L*a*b* colour system is an international standard developed in 1976. By mathematical conversion, seemingly indiscernible colour differences when observed by the human eye can be expressed as differing measured values of approximately the same magnitude. The tristimulus colour system comprises of three dimensional colour space where L* constitutes the ordinate and represents the brightness (L* from luminance, Figure 1), which ranges from black (0) to white (100). The abscissa ranges from green (negative a* values) to red (positive a* values) and the applicate ranges from blue (negative b* values) to yellow (positive b* values). The both chromatic axes range from -120 to 120. ∆L*, ∆a* and ∆b* values describe the colour differences between one reference standard value ($L^*_{standard}$, $a^*_{standard}$, $b^*_{standard}$) and a sample value (L^*_{sample}, a^*_{sample}, b^*_{sample}). Based on these values the colour difference (∆E) is calculated with Equation (1) which describes the linear distance of the sample and the standard in the three dimensional colour system. (Ohta and Robertson, 2005; Otterstätter, 1999) Therefore, the delta E value can be used to define the approved colour difference in processes (González-Manzano et al., 2008; Pathare et al., 2013).

Using L*a*b* values colour difference, ∆E can be calculated by using the following equations (Ohta and Robertson, 2005; Otterstätter, 1999)

$$\Delta E^* = \sqrt{(\Delta L^*)^2 + (\Delta a^*)^2 + (\Delta b^*)^2} \quad (1)$$

$$\Delta L^* = L^*_{sample} - L^*_{standard} \quad (2)$$

$$\Delta a^* = a^*_{sample} - a^*_{standard} \quad (3)$$

$$\Delta b^* = b^*_{sample} - b^*_{standard} \quad (4)$$

Likewise, other industries already use colour tolerances for ΔE values. For example, the evaluation of paper white (∆E = 3), which is stated in ISO 12647-7, is carried out with a spectrophotometer (Homann, 2010). The automotive industry also implemented a DIN (DIN 617-2) using 3 or 5 angle instrumentation, which is used by Audi for automatization of a process (Streitberger and Dössel, 2008). ∆E < 0.2 are not visible, 0.2 < ∆E < 0.5 are extremely poor visible, 0.5 < ∆E < 1.5 are poor visible, 1.5 < ∆E < 3.0 are visible and 3.0 < ∆E < 6.0 are strongly visible (Hellerich et al., 2010). Gierling, 2001 stated that a colour difference (∆E) below 1.0 is just visible to a professional, ∆E below 2.5 is not visible to a layperson and above 2.5 it is visible to a layperson. The purpose of this investigation is to compare standard methods for quality assertion with optical measurements of spectral properties in order to find out if this can be useful for further developments of at-line or in-line measurements to ensure high quality in the malt roasting process. The non-enzymatic browning, which is quantified with these methods, is dependent on the concentration of brown pigments in malt produced during pyrolysis of sugar (caramelization) as well as the reaction of the amino

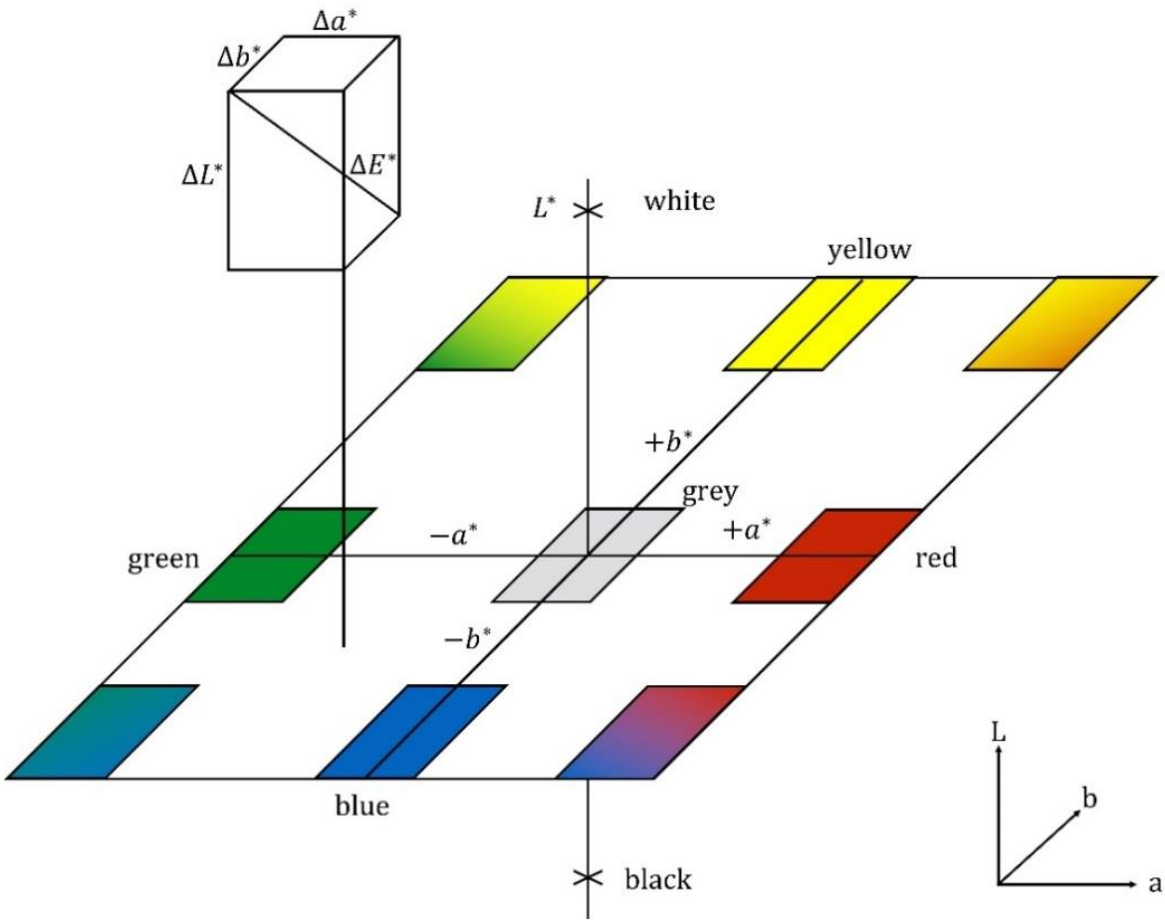

Figure 1. CIE- L*a*b* colour system: L* for the lightness from black (0) to white (100), a* from green (−) to red (+), b* from blue (−) to yellow (+) and quantifiable colour difference ΔE.
Source: Otterstätter (1999).

group of a free amino acid and the carbonyl group of a reducing sugar (Maillard reaction). These changes are reflected in altering chemical compositions and therefore varying vibrational modes. The goal is to investigate those changes in order to determine optimal roasting parameters. The Maillard reaction is a non-enzymatic browning reaction, which increases with temperatures (Labuza, 2005; Nie et al., 2013; O'Brien et al., op. 1998) due to increase in reactivity between the sugar and the amino group at higher temperature (Martins et al., 2000). By splitting off hydrocarbons, amino acids combine with reducing sugars to form a Schiff base. Some of these products (reductones, melanoidins) have a pro- or antioxidant effect and thus influence the oxidative stability of food (Cortés et al., 2010; Kanzler et al., 2017).

The formation of Maillard reaction products is influenced by temperature (Mohsin et al., 2018), time (Ćosović et al., 2010), water content (Faist et al., 2002; Yahya et al., 2014), pH-value (Kim and Lee, 2008; Kwak et al., 2005) and concentration of reaction partners (Spieleder, 2007; van Boekel, 2006). MRPs consist of aldehydes, acryl amides, dicarbonyls, ketones, heterocyclic amines and other compounds which are responsible for malt flavour and colour (Bravo et al., 2002; Cortés et al., 2010; Kanzler et al., 2017; Wang et al., 2011). An important product class is melanoidins, which are formed at the end of the Maillard reaction (Carvalho et al., 2014; Mohsin et al., 2018; Spieleder, 2007; van Boekel, 2006) and are mainly responsible for beer colour. Melanoidins with higher molecular weight are only formed at high temperatures. Melanoidin structures are largely unknown, with only a few being proposed. Hitherto, identification and characterisation of high-molecular, colour-intensive melanoidins are very challenging (Narziß et al., 2009). Additionally, another MRP 5-(hydroxymethyl) furfural is formed from hexose dehydration (Bertrand et al., 2018; Nursten, 2005). In this study, HMF is used as reference value for the intermediate stage of the Maillard reaction.

The other reaction involved in developing colour is sugar caramelization, which is the controlled

decomposition of sugars by pyrolysis. The process breaks down sugar molecules, evaporates the water and converts the remaining atoms into new flavours. In contrast to the Maillard reaction, here, no amino acid compounds are required. Moreover, it takes place at a higher temperature than the Maillard reaction, e.g. 110 for simple fructose and 180ºC for maltose. Caramelization of sugars produces both brown-coloured products with a typical caramel aroma and volatile aroma-active substances. In principle, the reactions correspond to those described in the Maillard reaction, except that the 3-deoxyosone is formed directly from the precursor hexose via 1,2-enolisation (Shahidi and Ambigaipalan, 2015).

Again, HMF is formed from hexoses and 2-furfural from pentoses (Kroh, 1994; van Boekel, 2006). HMF and furfural are intermediates formed during Maillard reaction due to 1,2 enolization (Martins et al., 2000). Additionally, acetic acid and vicinal diketones (diacetyl and 2,3-pentandione) formed after retro-aldolization are recognised as MRPs in malt (Coghe et al., 2006).

Furthermore, some of the compounds such as aliphatic alcohols, aldehydes, ketones, pyrroles, furans and pyrazines are identified in malted barley by gas chromatography (Beal and Mottram, 1994). Among the highlighted compounds, it is concluded that 3-methylbutanal and 2-methylbutanal increase dramatically in malt during roasting. Another study analysed fifteen Maillard products related to flavour development by roasting three different kinds of malt (Yahya et al., 2014). (Yahya et al., 2014) focused on the trend of maltol concentration in malt and the correlation with other compounds such as 2-furaldehyde, methyl-pyrazine, Isomaltol,2-furanmethanol, 2,3-Dihydro-3,5-dihydroxy-6-methyl-4H-pyran-4-one. Gupta et al., 2010 emphasized notable traces of β-Glucan, protein, fibers, arabinoxylans in by-products left after separating wort during the brewing process. Hydrolysis of starch carried out by malt enzymes during the malting process is also mentioned. The resulting fermentable sugars or simple sugars from this process are glucose, sucrose, fructose, maltose and dextrin (Gupta et al., 2010). Research on xylose content changes in malt is also conducted, concluding that xylose content in malt varies in a noticeable way (MacLeod et al., 1953). In this research, spectral changes in mid-infrared regions are investigated regarding biochemical, as well as colour changes during the roasting of malt. A correlation between reference values and spectral data were described by multi linear regressions.

MATERIALS AND METHODS

Kiln malt of the Avalon variety (provided by Palatia Malz GmbH, Wallertheim, Germany) was roasted in an eddy current laboratory roaster. Roasting test series were performed at different temperatures and roasting times. Roasting was stopped in 60 s intervals with a maximum exposure time of 780 s. For each specified roasting temperature (140, 160, 180, 200, 220ºC), 12 roasting test series were carried out. Roasted malt samples were then milled manually using a coffee grinder in order to get a small particle size distribution to measure as closely as possible to the process.

Additionally, the used diffuse reflection infrared Fourier transform (DRIFT) spectroscopy method required the utilization of small sample volumes. The malt samples were therefore analysed with DRIFT spectroscopy as grist. The roasted milled samples (grist) are displayed in Figure 2, starting in the left upper corner with 120 60 s and ending with 240ºC 780 s in the right lower corner. Each row showed a specific roasting temperature and the columns represent the roasting times 60 s, 120 s, 180 s, 240 s, 300 s, 360 s, 420 s, 480 s, 540 s, 600 s, 660 s, 720 s and 780 s.

Standard wort analysis

The basic chemical analysis for the characterisation of roasted malt samples was carried out by the Chair of Brewing and Bewerage Technology, Institute of Food Technology and Food Chemistry, Technical University of Berlin in accordance with the regulations of the Central European Brewing Analysis Commission (MEBAK) (Methner, 2018). Standardized and special reference methods were used in order to verify the roasting status. Malt was coarsely milled with an analytical mill (Brühler- MIAG A10, IKA Labortechnik), 75 g (90 roasted malt and 10% Pilsner malt) grist was mixed with 300ml double distilled water (55ºC) stirring constantly in a beaker. The grist was malted in a mash bath according to the following program: 5 min at 55, 5 min at 60, 20 min at 62, 25 min at 65, 20 min at 72 and subsequent heating-up to 78ºC. After reaching 78ºC, the beaker was taken out of the bath and rinsed with double distilled water. The total mass was filled with water to 450 g and subsequently filtered with a fluted filter (Whatmann Filter 597/2). 100 ml of the eluat was set aside as a sample before wort boiling for reference analysis regarding colour values (L*a*b* before wort boiling). The remaining 300 ml was cooked in the beaker under reflux for one hour, filtered with a fluted filter (Whatmann Filter 597/2) and cooled down before EBC colour of malt extract (MEBAK R-205.07.110 [2016-03] (Methner, 2018) 2.13.2. (Miedaner, 2002) and then L*a*b* was measured. Until further analysis, samples were kept frozen in storage. Solid samples were used for inductively coupled plasma optical emission spectroscopy (ICP-OES). High-performance liquid chromatography (HPLC) and Electron Spin Resonance (ESR) spectroscopy were carried out on the resulting eluat sample after boiling wort. Reduction capacity (Red. Cap. cf. MEBAK 2.16.1 (Miedaner, 2002)) and radical levels (T_{600} and ESR value cf. MEBAK 2.15.3 (Kunz et al., 2013; Methner et al., 2007; Miedaner, 2002; Uchida and Ono, 1996)) were determined according to MEBAK. The organic radical content of roasted malt was quantified using an optimized ESR spectroscopy method, patented (Kaneda et al., 2005) and described in a paper by (Takoi et al., 2003). The ESR measurement was optimized by the Technical University of Berlin, considering a method by (Cortés et al. 2010). Early Intermediates from Maillard reaction, for example α-dicarbonyls, such as 3-deoxy-hexosulose as well as HMF, were measured by High-Performance Liquid Chromatography with Diode-Array Detection (HPLC-DAD).

Determination of α-Dicarbonyl compounds via HPLC-DAD (Kanzler et al., 2017)

The quantification of α-Dicarbonyls (e.g. 3-DH) was carried out by high-performance liquid chromatography with diode-array detection after derivatization with *ortho*-Phenylendiamine (OPD). 5 ml of liquid

Figure 2. Milled roasted malt samples.

Table 1. HPLC DAD gradient of α-Dicarbonyl compounds.

Time (min)	Methanol (%)
0	20
5	20
35	60
40	60
45	20
55	20

sample was mixed with 1 ml 0.05 M OPD solution and derivatized at room temperature for 24 h. The solution was stored at – 18ºC until measurement. Prior to analysis, samples were filtered with a syringe filter (Nylon; 0.45 µM). A reverse phase column from Knauer (60-5 phenyl) was used for separation. The solvent gradient (methanol and water) was listed in Table 1. The flow rate for identifying α-Dicarbonyls was 0.5 ml/min. Calibration was performed with a standard. 40 µl standard mix or sample was injected. The temperature of the column oven was set to 35ºC. Detection and quantification was performed at 318 nm.

Determination of HMF via HPLC-DAD (Kanzler et al., 2017)

HMF served as indicator or marker substance for the formation of particular heterocyclic intermediates of the Maillard reaction. HMF was determined using an HPLC-DAD method described below (Kanzler et al., 2017). A reverse phase column from Knauer (60-5 phenyl) was used for separation. The solvent gradient consisted of methanol and phosphate buffer as listed in Table 2 at a flow rate of 0.5 ml/min. Calibration was performed with five different concentrations of a HMF standard. 20 µl standard mix or sample was injected. The temperature of the column oven was set to 35ºC. Detection and quantification was performed at 285 nm.

Determination of Iron entry via ICP-OES

The individual caused iron entry, dependent on roast status of grain samples, was measured using an ICP-OES system iCAP 6200 equipped with a CID 86 detector and an auto sampler from Thermo Scientific. Solid samples were digested beforehand by microwave. 0.25 g of solid samples was decomposed with 5 mL HNO_3 and 2 mL H_2O_2 and then placed in a Teflon vessel. The mixture was incubated for 1 h at room temperature and subsequently placed in a microwave oven for 1 h at 160ºC. Afterwards the sample was cooled for 30 min and filtered. All vessels and the filter were rinsed with demineralised water; further demineralised water was added to the solution until a total volume of 25 ml was reached for the following analyses via ICP-OES. Liquid samples were generated as described for the standard wort analyses. Subsequently, the defrosted wort samples were diluted with a dilution factor of 10 or 20, depending on wort colour, for the analyses via ICP-OE Avio 200 system equipped with a CCD detector and an autosampler. The iron concentration was determined by external calibration using ICP-OES with argon as carrier gas and emission lined at 238.2 nm and 259.9 nm.

Tristimulus colour measurement of L*a*b* values

The measurement of L*a*b* values was conducted using a

Table 2. HPLC DAD gradient of HMF.

Time (min)	Methanol (%)
0	5
5	5
15	20
20	20
25	95
35	95
40	5
45	5

photometer (Konica Minolta VC 5, illuminant D65 (DIN 6173-2) observer angle of 10º). The liquid samples (wort before and after boiling) were membrane filtered (25 mm Syringe filter, w/0.45 µm cellulose acetate). After required liquid calibration (0 and 100 % calibration) the samples were measured in 10 mm plastic cuvettes (triple determination). Grain kernels or milled grist were transferred into petri dishes for L*a*b* value determination. Due to the inhomogeneous solid samples (grain and grist), a fivefold determination with different rotation positioning of the petri dishes was performed.

Fourier-transformed infrared spectroscopy (FTIR) Spectroscopy

FTIR monitored the interaction of functional groups in chemicals molecules. The spectra were recorded with the FTIR spectrometer ALPHA-R from Bruker (Bruker Optics GmbH, Ettlingen, Germany) using the DRIFT (Diffuse Reflectant Infrared Fourier Transformation) module. Freshly milled malt was used for each measurement and the samples were scanned three times and the average ATR-FTIR spectrum was used for further analysis. The spectra, with 4 cm^{-1} resolution in the range from 4000 to 400 cm^{-1}, were recorded on OPUS software version 7.0 (Bruker Optics) and each sample was obtained by calculating the average of 24 scans. Gold was used as reference background spectra. The DRIFT sample compartment was cleaned before each sample was scanned. Freshly milled malt was used for each sample measurement. The resulting absorption spectra were cut off below 800 cm^{-1} and above 3700 cm^{-1}. Baseline correction (concave elastic band method, using 25 iterations and 30 baseline points) and smoothing (17 smoothing points) were performed, resulting in the spectra used for evaluation. Due to the complex biochemical matrix of the sample and therefore overlaying spectral changes, chemical standards were not measured. The spectra were evaluated by identifying peaks (b-f) and calculating the peak areas to the integral border.

Statistical Analysis

Regression analysis was a statistical evaluation method with the objective of describing a context by a function. The objective was to find a dependency between the dependent variable y and the co-variable x. Target quantity of the covariates could not be described exactly by the function, but were rather affected by disturbances. The target variable became a random variable, because its size depended on the distribution of the covariates. This meant that, without exception, the mean value of the covariates could be used to deduce the target variable. The distribution could not be predicted, therefore, the average was used for the calculation. The target variable could be described by a linear, quadratic or exponential function. The most frequently used regression model was linear and described by the following standard Equation (5):

$$y = \beta_0 + \beta_1 \cdot x_1 + \ldots + \beta_n \cdot x_n + \varepsilon_i \quad (5)$$

where ε_i is an error variable and β_n (with n=0, 1, 2,…) are unknown estimated parameters. For multiple linear regressions, multiple independent variables were used. A benchmark for linear relationship or the normal distribution was the coefficient of determination R^2. The coefficient of determination is expressed by the following Equation (6) (Fahrmeir et al., 2009):

$$R^2 = \frac{\sum_{i=1}^{n}(\hat{y}_i - \bar{y})^2}{\sum_{i=1}^{n}(y_i - \bar{y})^2} \quad (6)$$

$\hat{y} = \text{arithmetic mean of calculated values}$
$\bar{y} = \text{arithmetic mean of reference values}$
$y_i = \text{reference values}$

The number of degrees of freedom (df) was the number of values which remain in the final calculation of a varying statistic and it was calculated with Equation (7) for a linear regression (Kessler, 2005):

$$df = n - 2 \quad (7)$$

$n = \text{number of reference values}$

Additional coefficients of regression reduced the degree of freedom by one (Kessler, 2005). The degrees of freedom were used to calculate the residual standard error (RSE), which was the positive square root of the sum of the squared residuals divided by the degrees of freedom (Kessler, 2005), thus it was calculated by:

$$RSE = \sqrt{\frac{1}{df}\sum_{i=1}^{n}(y_i - \hat{y}_i)^2} \quad (8)$$

The independent variables were the calculated values of the areas b, c, d, e and f for all roasted samples. The independent variables were both temperature dependent ($T_{i\ldots m}$ for temperature ranging from i to m) and time dependent ($t_{i\ldots n}$ for roasting time ranging from i to n). Target variable corresponds to the reference values (EBC, iron content, TMAX value, HMF, 3-DH, reduction and L*, a*, b* values). For each reference value, a multiple regression model was created according to Equation (9) (Groß, 2003).

$$Abs. = f(T,t) \Rightarrow A = \begin{bmatrix} T_1t_1 & T_1t_2 & \ldots & T_1t_n \\ T_2t_1 & T_2t_2 & \cdots & T_1t_2 \\ \vdots & \vdots & & \vdots \\ T_nt_1 & T_1t_2 & \ldots & T_mt_n \end{bmatrix} \quad (9)$$

The R software (version 3.5.1, 2.07.2018) was used for pre-processing. For evaluation, a partial least square regression (PLSR) model was used and a scatterplot, a prediction plot and the coefficient of determination were generated.

RESULTS AND DISCUSSION

The resulting processed spectra of the samples were evaluated, concerning the changing areas of vibrational

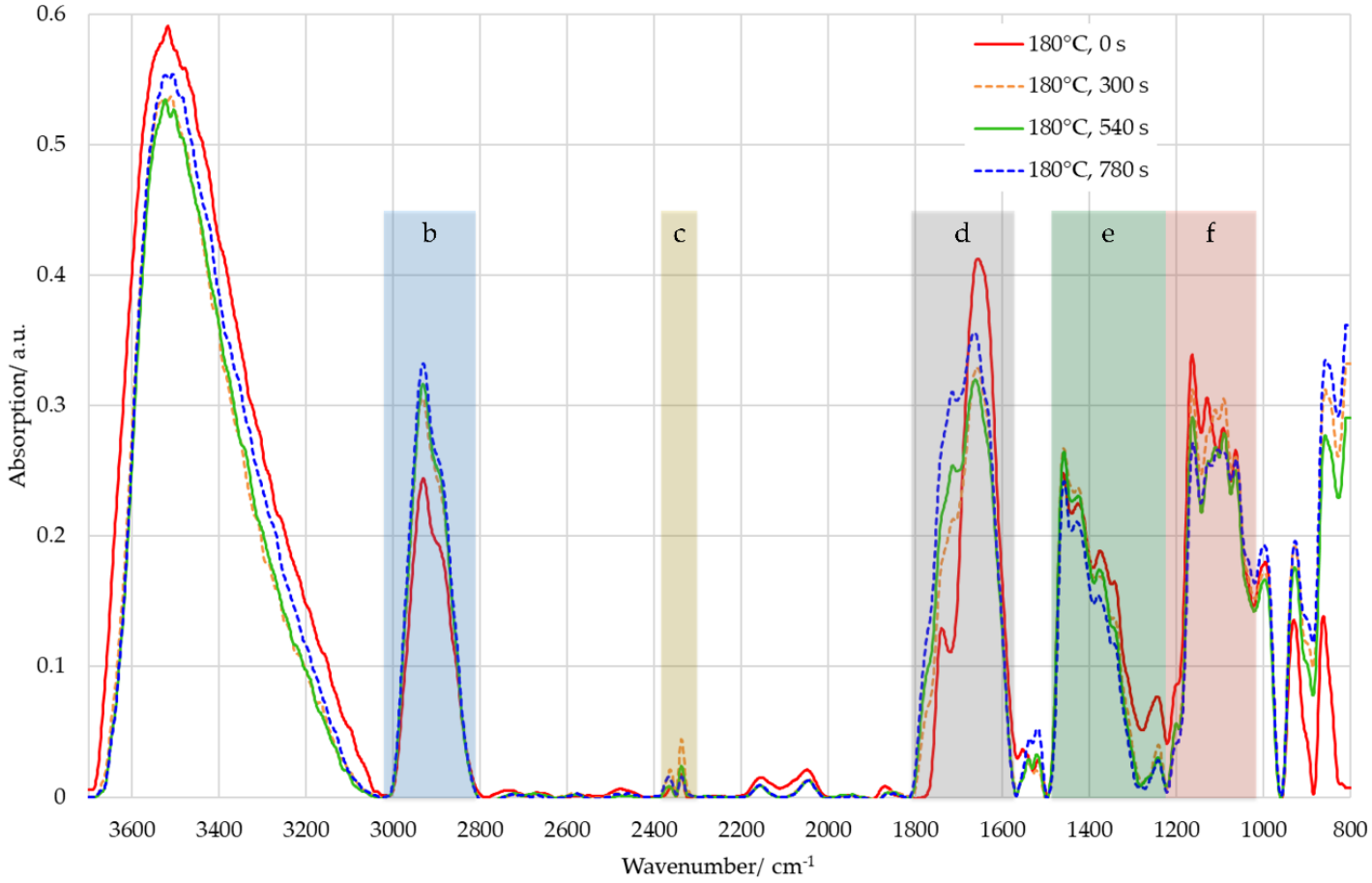

Figure 3. Processed spectra of roasted and unroasted malt with evaluated areas (variables) b-f.

changes during the roasting process. The first derivative was calculated in order to identify the spectral peak maxima, which represented relevant changes. As shown in Figure 3, the stretching vibration of water in between 3700- 3000 cm^{-1} changed due to the varying water concentration of the samples. However, the malt samples could have been influenced by the environment after milling and even during DRIFT measurement and therefore the range, where OH- absorption was visible, was not taken into account. The analysed peaks were in between 3027- 2787 cm^{-1} (b), 2362- 2307 cm^{-1} (c), 1807- 1567 cm^{-1} (d), 1500-1280 cm^{-1} (e) and 1218-962 cm^{-1} (f) (Figure 3). These ranges were used to calculate the areas underneath and then used as independent variables b, c, d, e and f for regression analysis.

The observed range for peak (b) was assigned to the stretching vibration of aliphatic carbon hydrogens (vC-H) at 2850- 2960 cm^{-1}, the stretching bond of amino groups (vN-H_3^+C-H) at 2600-3100 cm^{-1} and carboxyl acids at 2400-3300 cm^{-1} (Gunzler and Gremlich, 2003). Peak (c) was designated to the asymmetric stretching vibration of carbon dioxide (vCO_2 at 2349 cm^{-1}) (Groß, 2003) or aryl compounds (2309-2136 cm^{-1}) (Gunzler and Gremlich, 2003). In the region of 1807- 1567 cm^{-1} peak (d), the stretching vibration of carbonyl compounds (e.g. ketones, acids, esters, amides, etc.) as well as the deformation vibration of water (δH_2O) were located. Peak (e) was designated to the stretching vibration of aldehydes, deformation vibration of melanoidins or methyl groups. In the fingerprint region below 1500 cm^{-1} (peak f) each compound itself had a unique combination of peaks due to deformation vibrations generated by C-C and C-O interactions in ethers, alcohols, esters, etc. or stretching vibrations from C-N interactions from amines, amino acids or amides (Schmidt, 2000).

Table 3 lists the individual vibrations and the possible educts, intermediates or products which were influenced during roasting. In Figure 4, the results of standard wort analysis radical levels (ESR value cf. MEBAK 2.15.3 (Miedaner, 2002)) and the corresponding standard deviations were displayed as an example. The temperatures in between 140 to 180ºC showed a low ascent of organic radicals in contrast to the higher temperatures. The organic radical concentration

Table 3. Peak ranges and assigned vibrations and possible substances.

Peak label/ variable	Vibration
b	vC-H methyl group: 1-Deoxyosone and 3-Deoxyosone vC-H aromates (Gunzler and Gremlich, 2003); HMF (Nikolov and Yaylayan, 2011)
c	$v_{as}CO_2$ (2349) (Gunzler and Gremlich, 2003) or Aryl compounds (Gunzler and Gremlich, 2003)
d	vC=O and vC=N and vC=C Melanoidines (Cämmerer and Kroh, 1995; Rubinsztain et al., 1986) vOH carboxylic acid esters vC=O ketones vC=N carboxylic acid amides (Gunzler and Gremlich, 2003) δH_2O (Gunzler and Gremlich, 2003)
e	vC-C aldehydes: glucose Aryl-O-Ether (Gunzler and Gremlich, 2003) δOH melanoidins (Cämmerer and Kroh, 1995) δC-H methyl group: 1-Deoxyosone and 3-Deoxyosone (Cämmerer and Kroh, 1995; Ledl and Severin, 1978)
f	vC-O polysaccharides resulting from ether or carboxylic acids: aldoses (reducing sugar) or melanoidins (Cämmerer and Kroh, 1995) v_{as}C-C ketones (Gunzler and Gremlich, 2003) ethers (HMF -> aldehyd and ether) vN-H secundary amines (acrylamide and amino acids) or melanoidins (Cämmerer and Kroh, 1995) vN-H aromatic amines: pyridine (amadori product)

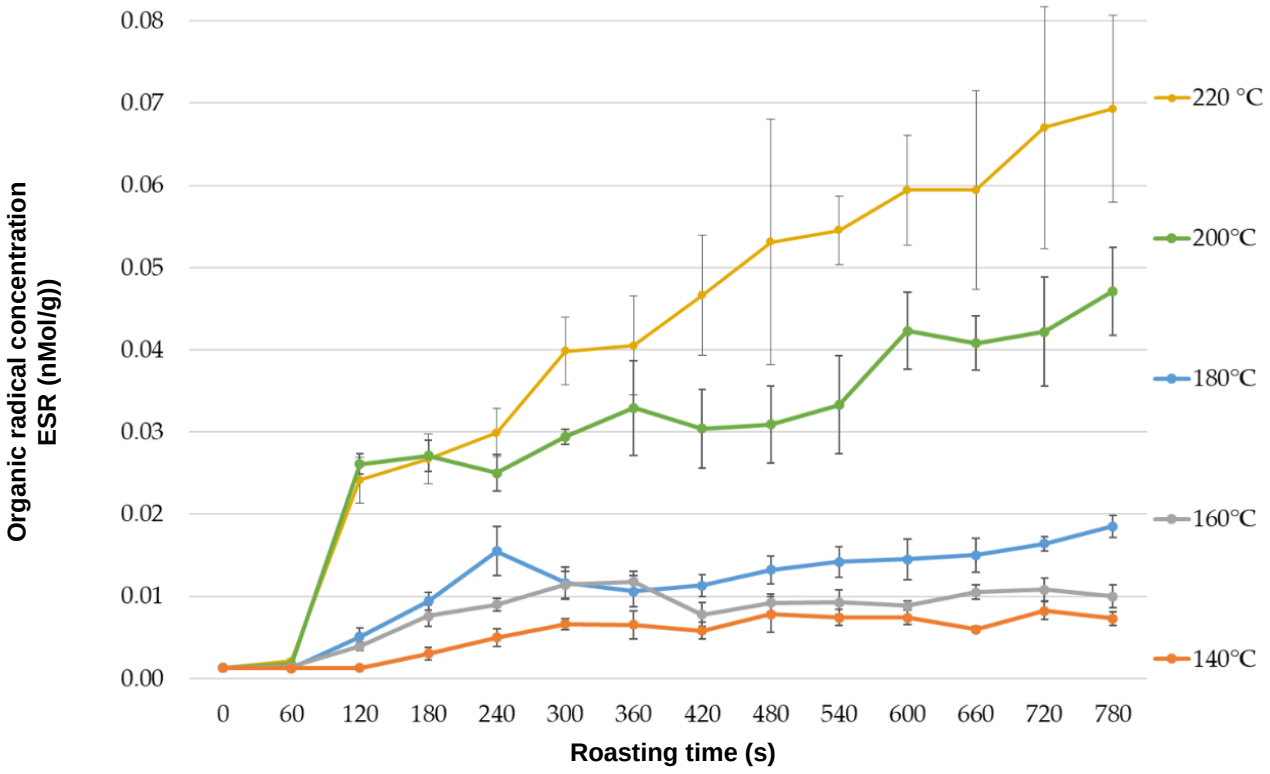

Figure 4. Organic radical concentration ESR over roasting time.

increased with roasting time and was highest for 220ºC.

Figure 5 exemplary displayed one resulting scatterplot matrix for the L* value of the grist (variable a), compared to the evaluated peaks (variable b- f). It was used to describe the correlation between the reference value (a) and variables b-f. The scatter plot matrix was used to

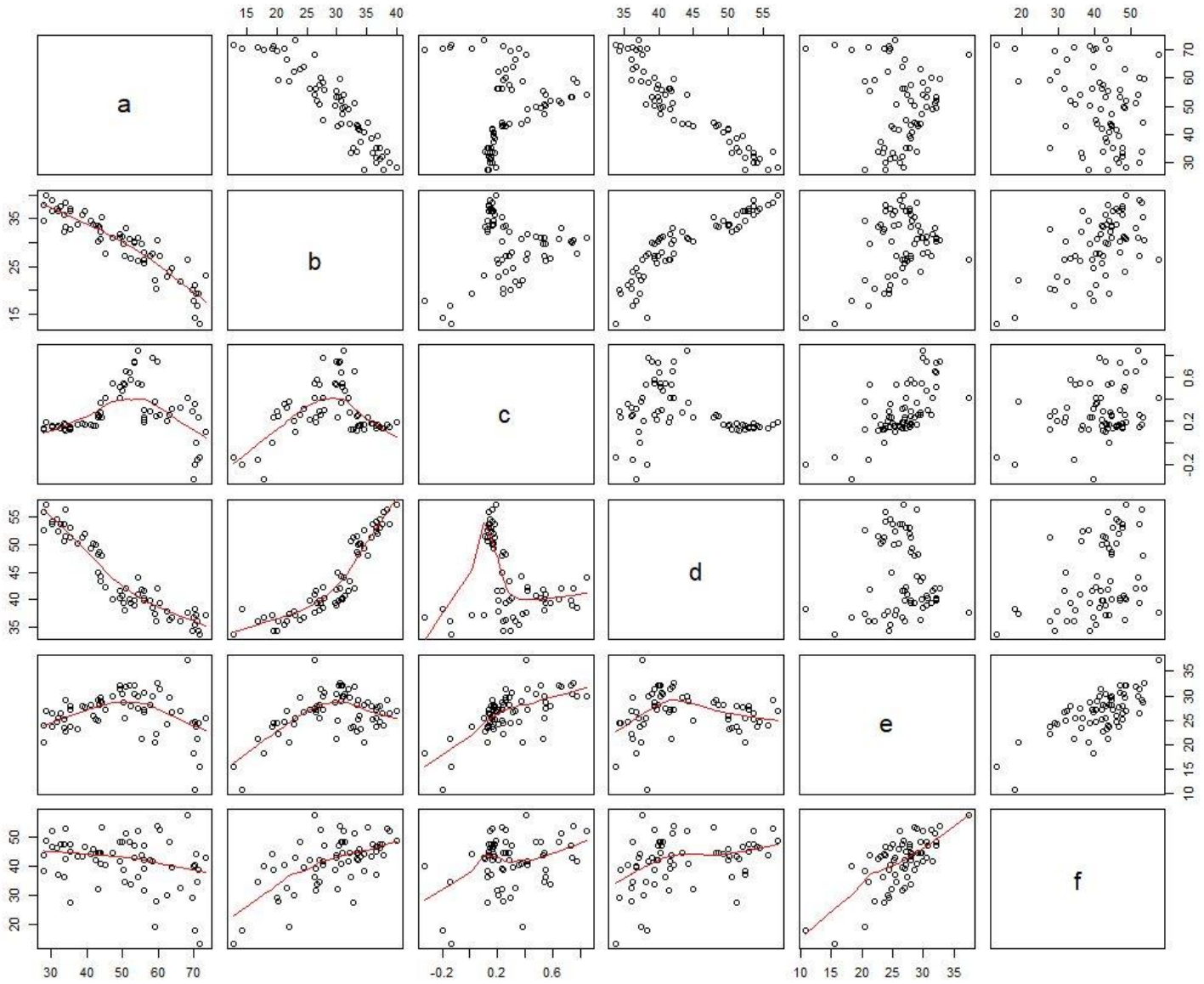

Figure 5. Scatter plot matrix for a= L*, grist and b-f= calculated peak areas.

select important variables and showed their relationship to each other. As shown in Figure 5, the L* value of grist (variable a) and the mid-infrared data in between 3027-2787 cm^{-1} (variable b) had a strong linear positive correlation. In contrast, variable (a) and (c) had no distinct linear relationship and showed a weak correlation as compared to variable (a) and (b).

Figure 6 (a) displayed the result of the multiple linear regression with the L*- values of the grist generated from the software. The prediction plot on the left side showed the predicted against the measured L*-values of grist. The linear regression was normally distributed, which could be seen on the right graphs (Figure 6 (b) – (e). The residuals vs fitted plot (Figure 6b) indicated that the residuals and the fitted values were uncorrelated, as they should be in a homoscedastic linear model with normally distributed errors. Most residuals were close to zero in contrast to the more extreme residuals which were far away from the rest. This indicated that the outliers were sample number 1 (unroasted), 19 (160ºC at 300s) and 34 (180ºC at 420 s). Those outliers were also visible in the normal Quantile-Quantile (Q-Q) plot and the scale location plot. In (Figure 6c) the standardized residuals were shown on the vertical axis and were compared to the theoretical quantiles in the Q-Q plot. The normal Q–Q plot compared the randomly, independent standard normal data to a standard normal population. As shown below, the data points essentially formed a straight line

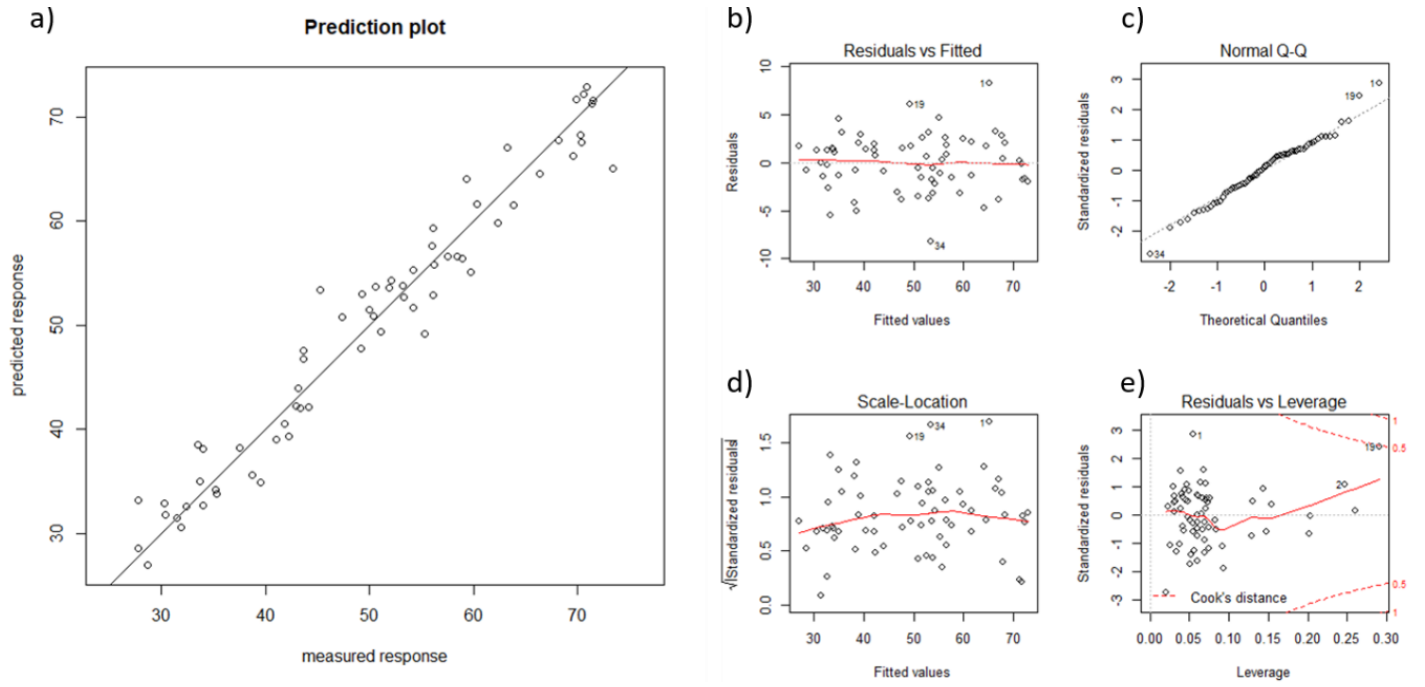

Figure 6. (a) Predicted vs. measured L* –values (grist), (b) residuals vs. fitted plot, c) normal QQ plot, (d) standardized residuals plot, (e) residuals vs Leverage plot with cook's distance.

which indicated that it was normally distributed. The Scale-Location plot (Figure 6d) showed that the residuals were spreaded equally along the predictor range of the L* grist variable. Since there was no any clear recognizable pattern of the measured L* grist values; the uniform variance was shown. The residuals vs leverage plot in (Figure 6e) showed that sample number 19 had a high influence on the regression line in contrast to sample number 1 and 2 (140°C at 60 s). Since the data sets were independent to each other and normally distributed, multiple linear regression was used. For further analysis and studies, the outliers, samples 1, 19 and 34, should not be considered.

In Figure 7, the calculated predicted data, on the basis of the independent variables b-f, was plotted against the measured reference values. On the left side in Figure 7, the prediction plot of the L*- value of grist was displayed and on the right side the prediction plot of the EBC value was shown. The measured L* values of grist ranged from 27.77 (beginning of roasting) to 73.37 (ending of roasting) and the coefficient of correlation was 0.953 with a standard deviation of 3.02. In contrast, the EBC values ranged from 30 to 780 and the coefficient of determination was 0.845 with a standard deviation of 78.19. The outliers in the EBC regression model, especially at the end of the roasting, could be seen at values above 580.

In Table 4, the resulting coefficients of determination (R^2) as well as the residual standard error (RSE) and the corresponding degrees of freedoms (df) were summarised. For the multiple linear regressions, all independent variables b-f were used to calculate the coefficients of determination. The results were compared to the linear regression models using variables (b), (f) separately as well as both.

Variable b showed a high correlation to referenced colour values and was, therefore, individually examined. In order to show the contribution of a second measured wavelength, variable f was taken as an example. The comparative low R^2, used together with variable (b), enhanced the model and additionally, proved that not all used variables had the same contribution to the model fit if taken into account. Due to the possible photometric measurement of the data, just the two variables (b) and (f) were taken as example. With measured variable (b) only, the coefficient of determination would not be robust for further implementing in roasting processes. The same applied for variable (f). In contrast, if both were included, significant coefficients of determination were calculated and therefore could be used in future developments of process automatization. However, the L*-, a*- and b*-values taken on their own did not give any information about the true colour. Therefore, the colour difference value ΔE was calculated for L*a*b* values of grain, grist, wort before and after boiling by using the unroasted sample as standard. The resulting margin of the values, R^2, df and RSE were summarized in Table 5. The ΔE values for grain varied in between 3.11 and 46.14 and

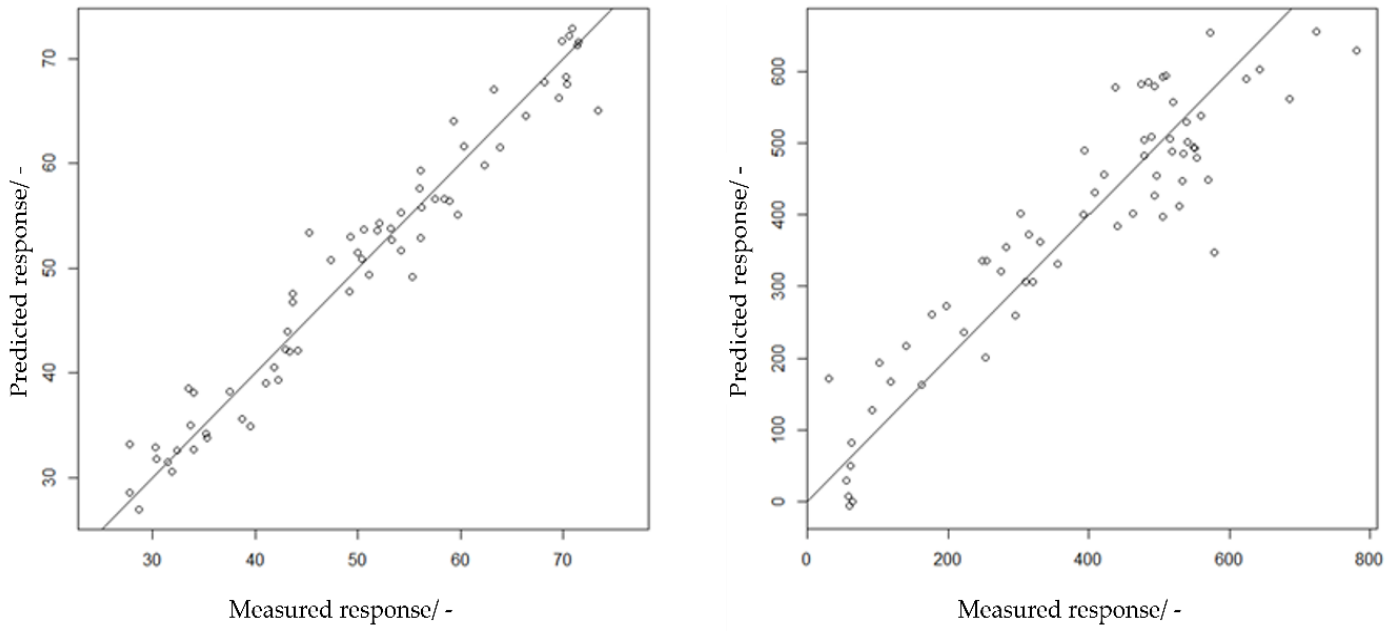

Figure 7. Comparison of prediction plot of (left) L value of grist and (right) EBC value.

Table 4. Calculated R^2 with varying dependent variable a (reference values) in the first column, covariables b-f (peak areas), designated RSE and df.

Variable a	Variables b, c, d, e and f			Variables b and f			Variable b			Variable f		
	df	R^2	RSE	df	R^2	RSE	df	R^2	RSE	df	R^2	RSE
EBC	59	0.845	78.190	62	0.835	78.800	63	0.766	92.990	63	0.117	180.700
Iron concentration	53	0.484	277.300	56	0.002	375.200	57	0.001	372.200	57	0.000	372.300
T_{600}	58	0.629	1.499	61	0.510	1.680	62	0.462	1.746	62	0.065	2.303
HMF	42	0.867	0.233	45	0.806	0.271	46	0.681	0.344	46	0.122	0.571
3-DH	42	0.728	630.300	45	0.693	646.900	46	0.597	733.100	46	0.058	1121.000
Red. Capacity	58	0.600	103.400	61	0.566	105.100	62	0.543	107.000	62	0.121	148.400
ESR	60	0.841	0.008	63	0.675	0.010	64	0.629	0.011	64	0.102	0.017
L*, grain	60	0.883	2.631	63	0.875	2.657	64	0.806	3.288	64	0.119	7.000
a*, grain	60	0.667	0.552	63	0.640	0.561	64	0.620	0.571	64	0.140	0.860
b*, grain	60	0.826	1.337	63	0.700	1.711	64	0.601	1.958	64	0.053	3.017
L*, grist	60	0.953	3.021	63	0.930	3.597	64	0.842	5.344	64	0.110	12.690
a*, grist	60	0.707	0.988	63	0.472	1.293	64	0.457	1.301	64	0.103	1.672
b*, grist	60	0.767	1.928	63	0.335	3.174	64	0.270	3.300	64	0.014	3.835
L*, wort before boiling	60	0.881	9.111	63	0.811	11.190	64	0.756	12.620	64	0.123	23.940
a*, wort before boiling	60	0.438	10.150	63	0.122	12.390	64	0.088	12.520	64	0.002	13.100
b*, wort before boiling	60	0.821	12.780	63	0.803	13.080	64	0.738	14.980	64	0.107	27.620
L*, wort after boiling	60	0.878	8.152	63	0.800	10.200	64	0.842	5.344	64	0.131	21.080
a*, wort after boiling	60	0.515	8.959	63	0.282	10.630	64	0.227	10.950	64	0.012	12.380
b*, wort after boiling	60	0.876	10.860	63	0.837	12.130	64	0.779	14.030	64	0.124	27.910

resulted in R^2 (b,c,d,e,f (ΔE, grist))=0.699 and a RSE of 1.927. The coefficient of determination for the colour difference of grist was 0.956 with a standard error of 2.722, which meant that there was a very strong correlation between the ΔE values and the analysed MIR data. The coefficient of determination of ΔE for wort

Table 5. Value margin of ΔE values and corresponding coefficients of determination by using variables b-f

Variable	df	R^2	RSE	Values margin of ΔE
Δ E, grain	59	0.699	1.927	3.11-46.14
Δ E, grist	59	0.956	2.722	27.07-42.26
Δ E, wort before boiling	59	0.917	6.743	20.53-100.32
Δ E, wort after boiling	59	0.910	8.055	19.7-106.09

Table 6. Coefficients of determination for EBC, HMF, L*, grist and Δ E, grist with added temperature (g) and time (h) as variables

Variable	Statistical analysis	EBC	HMF	L*, grist	Δ E, grist
g	df	63	46	64	63
	R^2	0.3202	0.4622	0.4836	0.4501
	RSE	158.500	0.4471	9.666	9.337
h	df	63	46	64	63
	R^2	0.4621	0.0750	0.4081	0.3967
	RSE	141.000	0.5863	10.350	9.780
b, c, d, e, f, g, h	df	57	40	58	57
	R^2	0.9068	0.9093	0.9741	0.9742
	RSE	61.690	0.197	2.273	2.127
b, g	df	62	45	63	62
	R^2	0.7661	0.7579	0.8568	0.8619
	RSE	93.720	0.303	5.130	4.717
b,h	df	62	45	63	62
	R^2	0.8365	0.6814	0.8764	0.8865
	RSE	78.360	0.348	4.766	4.277
b,g,h	df	61	44	62	61
	R^2	0.8590	0.8087	0.9335	0.9323
	RSE	73.350	0.273	3.524	3.329
b,f,g,h	df	60	43	61	62
	R^2	0.8818	0.8791	0.9655	0.8467
	RSE	67.730	0.219	2.558	4.969

before (R^2=0.917) and after boiling (R^2=0.910) were similar due to the sample treatment. The wort before boiling was cooked under reflux for one hour and filtered to obtain the wort after boiling, which was done to compare the sample (wort after boiling) as close as possible to the brewing process itself, though the colour of the sample did not change a lot during the second cooking.

Additionally, roasting temperature and time could be used for further stabilizing the model. In most roasting processes, time and temperature were already available data sets and if incorporated in the model, the coefficient of determination could be further improved. If the multi-linear regression model, using the existing variables b-f, was extended with variable (g) as temperature and variable (h) as time, the coefficients of determination for EBC values could be enhanced from R^2(b,c,d,e,f (EBC)) = 0.8451 to R^2(b,c,d,e,f,g,h (EBC)) = 0.9068 (Table 6). The coefficients of determination for HMF and L*, grist were increased from R^2(b,c,d,e,f (HMF))= 0.8761 and R^2(b,c,d,e,f (L*, grist)) = 0.9527 to R^2(b,c,d,e,f,g,h (HMF)) = 0.9093 and R^2(b,c,d,e,f,g,h(L*,grist)) = 0.9741. A photometric measurement of two wavelengths, or in our case variable (b) and (f), could be combined for prediction models of the EBC value, Δ E values, HMF concentration or the L*- value of grist. By using the temperature (g), time (h), the ranges 3027- 2787 cm^{-1} (b) and 1219- 962 cm^{-1} (f) as variables, the calculated coefficients of determination were R^2(b,f,g,h (EBC)) = 0.8818, R^2(b,f,g,h (HMF)) = 0.8791, R^2(b,f,g,h (L*,grist)) = 0.9655 and R^2(b,f,g,h (ΔE,grist))= 0.8467.

The coefficients of determination for all five variables

varied in between R^2(b,c,d,e,f(a*,wort before)) = 0.438 for reference a*- value of the wort before boiling and R^2(b,c,d,e,f(L*,grist)) = 0.953 for reference L*- value of the grist. Some coefficients of determination showed a weak correlation between the independent variables and the reference values, like iron concentration (R^2 = 0.484), Tmax (R^2 = 0.629), 3-DH (R^2= 0.728) and the reduction capacity (R^2 = 0.600). Similarly, the coefficient of determination for a* of grain (R^2 = 0.667), grist (R^2= 0.707), wort before boiling (R^2= 0.438) and after boiling (R^2= 0.515) as well as the b* value of grist (R^2= 0.767) did not show a strong correlation.

In contrast, strong correlations were found for HMF R^2(b,c,d,e,f(HMF)) = 0.867, ESR R^2(b,c,d,e,f(ESR)) = 0.841 and L* R^2(b,c,d,e,f(L*,grist)) = 0.953. Considering the variables separately, the coefficients of determination for L*, grist were R^2 (b(L*, grist))= 0.842 and R^2(f(L*,grist))= 0.110. The correlation of the reference value and the variable (b) would mostly result in a weak correlation, except for the correlation between the L*-value of grain, grist and the wort before boiling. As shown in Table 4, range of R^2 for variable (f) was in between R^2 (f(a*, grain)=0.140 and R^2(f(Iron conc.))=0. Therefore, the variable (f) itself resulted in no correlation for all evaluated reference values. The results for variable (b) varied in between R^2 (b(iron conc.))= 0.001 and R^2 (b (L*, grist)) = 0.842. The coefficients of determination for L*- value of grist overall showed strong correlations. By using the EBC value, with only one variable for the multi linear regression, the resulting correlation was weak ranging from R^2 (f(EBC))= 0.117 to R^2(b(EBC))=0.766. However, taken both variables into account, a good correlation with R^2 (b), (f) (EBC))=0.835 could be achieved. The significance of the evaluated variables could be seen, if all variables were used to calculate the coefficient of determination. For the EBC value, the coefficient of determination was increased by 0.01 up to R^2 (b,c,d,e,f (EBC))= 0.845. Therefore, variables c, d and e all together did not show an impact on the correlation.

The correlation of the grinded samples (grist values) displayed the highest correlation by using the colour reference values L*a*b. Overall, most colour reference values showed a good coefficient of determination utilizing all variables: EBC (R^2= 0.845), L*, grain (R^2= 0.883), b*, grain (R^2= 0.826), L*, grist (R^2= 0.953), L*, wort before boiling (R^2= 0.881), b*, wort before boiling (R^2= 0.821), L*, wort after (R^2= 0.878), b*, wort after (R^2= 0.876).

As displayed in Figure 6, the data sets 1, 19 and 34 were outliers. If left out, the resulting coefficient of determination for the L-value of grist R^2 (b,c,d,e,f) increased from 0.953 to 0.969. Due to the roasting process test, the samples were roasted beyond their optimal colour and flavour and therefore, the model could be further optimized by using only pertinent values before and right after the stop of the roasting. This could be further used as a basis for a photometric measurement in malt roasting. However, the methodology presented must be an at-line method only at this stage, due to the used MIR spectroscopy. The application as inline measurement would require a system that can cope with elevated temperatures, which is not given with most MIR measurements. Considering the reference values, the correlation of the grinded samples (grist values) displayed the highest correlation by using the colour reference values L*a*b* or ΔE. This was due to spectral data, which was used as basis to calculate the evaluated areas. These data were obtained from the FTIR measurement of grist as well as the reference values. If the sample was further processed, the evaluated reference values still resulted in comparably high correlations for the L*- values. The dependent variable a (e.g. HMF, ESR or EBC) was derived from liquid sample measurements and compared to grinded sample (grist) measurements.

In general, the MIR data obtained in region 3027- 2787 (variable b) and 962-1218 cm^{-1} (variable f) showed the strongest correlation. The high correlation of variable (b) could be due to the signal of the stretching vibration (vC-H) of aromates like HMF or 1-Deoxyosone and 3-Deoxyosone (Ledl and Severin, 1978). Peak (c) could be designated to the asymmetric stretching vibration of carbon dioxide (vCO_2 at 2349cm^{-1}) (Groß, 2003) or possibly a little influence of aryl compounds (2309-2136cm^{-1}) (Gunzler and Gremlich, 2003), but due to the volatility of CO_2, no strong correlation could be found. The bands in range d (1807- 1567 cm^{-1}) might be due to many different stretching vibrations of carbonyl compounds like ketones, acids, esters, amides, etc. (Gunzler and Gremlich, 2003). The deformation vibration of water (δH_2O) was also located in that region (Gunzler and Gremlich, 2003) and might vary due to the different roasting degrees of the samples. Based on the simultaneous complex reactions during Maillard reaction, the composition and degradation of compounds could result in a non-distinct overlapping of vibrations. In the fingerprint region below 1500 cm^{-1}, each compound itself had a unique combination of absorption bands due to deformation vibrations generated by C-C and C-O interactions in ethers, alcohols, esters, etc. or stretching vibrations from C-N interactions from amines, amino acids or amides (Schmidt, 2000). Variable (f) (1218- 962 cm^{-1}) was located in that range and designated to stretching vibrations (vC-O) of polysaccharides resulting from ethers or carboxylic acids, like aldoses, or melanoidins (Cämmerer and Kroh, 1995) or the stretching vibration of ketones (v_{as}C-C) (Gunzler and Gremlich, 2003). This could explain the high correlations of variable (f) to reference factors, like colour values. During the roasting process of malt, sugars were degraded in Maillard reaction and other intermediates or melanoidins were formed (Cämmerer and Kroh, 1995).

Variable (f) could be designated to the stretching vibration of polysaccharides (vC-O), carboxylic acids

(aldoses), alcohol (vC-O), esters, and ethers as well as the stretching vibration of amines. Especially several bands in between 900 and 1200 cm^{-1} were assigned to the C1-0-C4 stretching mode of maltose. Sekkal et al. observed the 1-4 linkage in α-D-glucopyranosyl-(1→4)-D-glucopyranose at 922 cm^{-1} (Sekkal et al., 1995).

Conclusion

The study presented that developed partial least square regression models can be used as basis for implementation of process control via mid-infrared spectroscopy in future. HMF, color related and ESR values of the roasted malt in particularly are correlated with spectral data and therefore can be used as first approach in further studies. Most of the reference values use methods which require time-consuming sample handling and preparation. As a consequence, the data handling is done manually and it creates difficulty to implement in an automated process control. If a cost saving photometric approach measures only two selected ranges and utilizes both recorded time (h) and temperature (g) to enhance the prediction of a wanted reference value, an automated roasting of malt can be included cost effectively in future. By further enhancing the model, one or more actuating variables can be used for process control and as a basis to calculate a stop criterion of malt roasting. L*a*b*- values can be measured photometric and be standardized for each variety of the roasting process. With acceptable tolerance levels, e.g. confidence intervals of ∆E values, roasting of malt can be calibrated and taken advantage of for automatization.

ACKNOWLEDGMENTS

The authors are grateful to Clemens Kanzler, Department of Food Chemistry and Analytics, Institute of Food Technology and Food Chemistry, Technische Universität Berlin for his kind help and analytical support to acsertain α Dicarbonyl compounds and HMF and also to Bestmalz (Wallertheim, Rheinland-Pfalz, Germany Thomas Schuhmacher, René Schneider and Danny Schmitt) for providing sample material. Additionally, to Bundesministerium fur wirtschaft and Energie (BMWi) and the Arbeitsgemeinschaft industrieller Forschungsvereinigungen (AiF, ZF4013933DB7) for funding the research work.

CONFLICT OF INTERESTS

The authors declare no conflict of interest.

REFERENCES

Bamforth CW (2009). Beer: A quality perspective. Handbook of alcoholic beverages. Elsevier Academic, Amsterdam.

Bamforth CW (2017). Progress in Brewing Science and Beer Production. Annual Review of Chemical and Biomolecular Engineering 7(8):161-176.

Beal AD, Mottram DS (1994). Compounds contributing to the characteristic aroma of malted barley. Journal of Agricultural and Food Chemistry 42(12):2880-2884.

Bertrand E, El Boustany P, Faulds CB, Berdagué JL (2018). The Maillard Reaction in Food: An Introduction. In: Reference Module in Food Science. Elsevier.

Bishop LR (1950). Proposed Revision of the Lovibond “52 Series” of Glass Slides for the Measurement of the Colour of Worts and Beers. Journal of the Institute of Brewing 56(6):373-382.

Bishop LR (1966). European Brewery Convention Tests of the E.B.C. Colour Discs for Wort and Beer. Journal of the Institute of Brewing 72(5):443-451.

Bravo A, Sanchez B, Scherer E, Herrera J, Rangel-Aldao R (2002). α-Dicarbonylic compounds as indicators and precursors of flavor deterioration during beer aging. Technical quarterly - Master Brewers Association of the Americas pp. 13-23.

Cämmerer B, Kroh LW (1995). Investigation of the influence of reaction conditions on the elementary composition of melanoidins. Food Chemistry 53(1):55-59.

Carvalho DO, Correia E, Lopes L, Guido LF (2014). Further insights into the role of melanoidins on the antioxidant potential of barley malt. Food Chemistry 160:127-133.

Coghe S, Gheeraert B, Michiels A, Delvaux FR (2006). Development of Maillard Reaction Related Characteristics During Malt Roasting. Journal of the Institute of Brewing 112(2):148-156.

Contreras-Jiménez B, Del Real A, Millan-Malo BM, Gaytán-Martínez M, Morales-Sánchez E, Rodríguez-García ME (2019). Physicochemical changes in barley starch during malting. Journal of the Institute of Brewing 125(1):10-17.

Cortés N, Kunz T, Suárez AF, Hughes P, Methner FJ (2010). Development and Correlation between the Organic Radical Concentration in Different Malt Types and Oxidative Beer Stability. Journal of the American Society of Brewing Chemists 68(2):107-113.

Ćosović B, Vojvodić V, Bošković N, Plavšić M, Lee C (2010). Characterization of natural and synthetic humic substances (melanoidins) by chemical composition and adsorption measurements. Organic Geochemistry 41(2):200-205.

Cozzolino D, Roumeliotis S, Eglinton J (2013). Prediction of starch pasting properties in barley flour using ATR-MIR spectroscopy. Carbohydrate Polymers 95(1):509-514.

Cozzolino D, Schultz D, Allder K, Eglinton J, Roumeliotis S (2014). Feasibility study on the use of attenuated total reflectance mid-infrared spectroscopy for the analysis of malt quality parameters in wort. Journal of the Institute of Brewing 120(4):385-389.

Czuchajowska Z, Szczodrak J, Pomeranz Y (1992). Characterization and Estimation of Barley Polysaccharides by Near-Infrared Spectroscopy. I. Barleys, Starches and Bdglucans. American Association of Cereal Chemistry 69(4):413-418.

Hans ME (2009). Handbook of brewing: Processes, technology, markets. Wiley-VCH-Verl., Weinheim.

Fahrmeir L, Kneib T, Lang S (2009). Regression: Modelle, Methoden und Anwendungen, 2nd edn. Statistik und ihre Anwendungen. Springer-Verlag Berlin Heidelberg, Berlin, Heidelberg.

Faist V, Lindenmeier M, Geisler C, Erbersdobler HF, Hofmann T (2002). Influence of molecular weight fractions isolated from roasted malt on the enzyme activities of NADPH-cytochrome c-reductase and glutathione-S-transferase in Caco-2 cells. Journal of Agricultural and Food Chemistry 50(3):602-606.

Farber M, Barth R (2019). Mastering brewing science: Quality and production. John Wiley & Sons, Inc, Hoboken, NJ.

Fox GP, Onley-Watson K, Osman A (2002). Multiple Linear Regression Calibrations for Barley and Malt Protein Based on the Spectra of Hordein. Journal of the Institute of Brewing 108(2):155-159.

Gajdoš KJ, Benković M, Bauman I (2015). Classification and Processing Optimization of Barley Milk Production Using NIR Spectroscopy, Particle Size, and Total Dissolved Solids Analysis. Journal of Chemistry Article ID 896051 https://doi.org/10.1155/2015/896051

Gierling R (2001). Farbmanagement: Profilerstellung für Ein- und Ausgabegeräte; Farbmanagement mit Grafik- und DTP-Programmen; Lösungen für Print und Web, 1st edn. mitp-Verl., Bonn.
González-Manzano S, Santos-Buelga C, Dueñas M, Rivas-Gonzalo JC, Escribano-Bailón T (2008). Colour implications of self-association processes of wine anthocyanins. European Food Research and Technology 226(3):483-490.
Goupy P, Hugues M, Boivin P, Amiot MJ (1999). Antioxidant composition and activity of barley (Hordeum vulgare) and malt extracts and of isolated phenolic compounds. Journal of the Science of Food and Agriculture 79(12):1625-1634.
Groß J (2003). Linear regression. Lecture Notes in Statistics, vol 175. Springer, Berlin.
Gunzler H, Gremlich HU (2003). IR-Spektroskopie: Eine Einfuhrung, 4th edn. Wiley-VCH, Weinheim.
Gupta M, Abu-Ghannam N, Gallaghar E (2010). Barley for Brewing: Characteristic Changes during Malting, Brewing and Applications of its By-Products. Comprehensive Reviews in Food Science and Food Safety 9(3):318-328.
Hellerich W, Harsch G, Haenle S (2010). Werkstoff-Führer Kunststoffe: Eigenschaften, Prüfungen, Kennwerte, 10th edn. Carl Hanser Fachbuchverlag, s.l.
Homann JP (2010). Digital Color Management: Principles and Strategies for the Standardized Print Production, 1st edn. X.media.publishing. Springer Berlin, Berlin.
Jacob F (ed) (2016) MEBAK brautechnische Analysenmethoden - Rohstoffe: Rohfrucht, Gerste, Malz, Hopfen und Hopfenprodukte: Methodensammlung der Mitteleuropäischen Brautechnischen Analysenkommission. Selbstverlag der MEBAK, Freising-Weihenstephan.
Kaneda H, Takoi K, Nishita N, Yoshimura J, inventors; Sapporo Breweries Ltd (2005). Method of evaluating green malt qualities by electron spin resonance spectrometry and method of evaluating malt qualities: U.S. Patent (6952098 B2).
Kanzler C, Schestkowa H, Haase PT, Kroh LW (2017). Formation of Reactive Intermediates, Color, and Antioxidant Activity in the Maillard Reaction of Maltose in Comparison to d-Glucose. Journal of Agricultural and Food Chemistry 65(40):8957-8965.
Kessler W (2005). Multivariate Datenanalyse in der Bio- und Prozessanalytik: Mit Beispielen aus der Praxis. Wiley-VCH, Weinheim.
Kim JS, Lee YS (2008). Effect of reaction pH on enolization and racemization reactions of glucose and fructose on heating with amino acid enantiomers and formation of melanoidins as result of the Maillard reaction. Food Chemistry 108(2):582-592.
Kroh LW (1994) Caramelisation in food and beverages. Food Chemistry 51(4):373-379.
Kunz T, Müller C, Methner FJ (2013). EAP determination and beverage antioxidative IndeX (BAX) - Advantageous tools for evaluation of the oxidative flavour stability of beer and beverages (Part 1). Brewing Science 66:12-22.
Kwak EJ, Lee YS, Murata M, Homma S (2005). Effect of pH control on the intermediates and melanoidins of nonenzymatic browning reaction. LWT - Food Science and Technology 38(1):1-6.
Labuza TP (2005). Maillard reactions in chemistry, food and health. Woodhead Publishing Limited, Cambridge [England].
Ledl F, Severin T (1978). Brunungsreaktionen von Pentosen mit Aminen. Z Lebensm Unters Forch 167:410-413. https://doi.org/10.1007/BF01459865
MacLeod AM, Travis DC, Wreay DG (1953). Studies On The Free Sugars Of The Barley Grain. Journal of the Institute of Brewing 59(2):154-165.
Mallet J (2014). Malt: A Practical Guide from Field to Brewhouse. Brewing Elements, v. 5. Brewers Publications, Boulder, CO.
Martins SI, Jongen WM, van Boekel MA (2000). A review of Maillard reaction in food and implications to kinetic modelling. Trends in Food Science andTechnology 11(9-10):364-373.
Methner FJ (ed) (2018). MEBAK- Raw Materials: Adjuncts Barley Malt Hops and Hop Products. Self- published by MEBAK, Freising-Weihenstephan.
Methner FJ, Kunz T, Schön T (eds) (2007). Application of optimized methods to determine the endogenous anti-oxidative potential of beer and other beverage. Fachverlag Hans Carl, Nürnberg, Germany.
Miedaner H (ed) (2002). Brautechnische Analysenmet.hoden: Methodensammlung der Mitteleuropäischen Brautechnischen Analysenkommission (MEBAK), 4th edn. Selbstverl. der MEBAK, Freising-Weihenstephan.
Mohsin GF, Schmitt FJ, Kanzler C, Dirk Epping J, Flemig S, Hornemann A (2018). Structural characterization of melanoidin formed from d-glucose and l-alanine at different temperatures applying FTIR, NMR, EPR, and MALDI-ToF-MS. Food Chemistry 245:761-767. https://doi.org/10.1016/j.foodchem.2017.11.115
Narziß L, Back W, Burberg F (2009). Die Technologie der Würzebereitung, 8th edn. Die Bierbrauerei, / Ludwig Narziß; Werner Back; Bd. 2. Wiley-VCH, Weinheim.
Nie S, Huang J, Hu J, Zhang Y, Wang S, Li C, Marcone M, Xie M (2013). Effect of pH, temperature and heating time on the formation of furan in sugar–glycine model systems. Food Science and Human Wellness 2(2):87-92.
Nikolov PY, Yaylayan VA (2011). Thermal decomposition of 5-(hydroxymethyl)-2-furaldehyde (HMF) and its further transformations in the presence of glycine. Journal of Agricultural and Food Chemistry 59(18):10104-10113.
Nursten HE (2005). Maillard Reaction. Royal Society of Chemistry, Cambridge.
O'Brien J, Nursten HE, Crabbe MJC, Ames JM (op. 1998). The Maillard reaction in foods and medicine: [proceedings of the 6th International symposium on the Maillard reaction, held at the Royal College of Physicians, London, UK, 27-30 July 1997]. Special publication, Vol. 223. Royal Society of Chemistry, Cambridge.
Ohta N, Robertson AR (2005). Colorimetry: Fundamentals and applications. Wiley-IS&T series in imaging science and technology. J. Wiley, Chichester, West Sussex, England, Hoboken, NJ, USA.
Otterstätter G (1999). Coloring of food, drugs, and cosmetics. Food Science and Technology, Vol. 91. Dekker, New York.
Pathare PB, Opara UL, Al-Said FAJ (2013). Colour Measurement and Analysis in Fresh and Processed Foods: A Review. Food Bioprocess Technology 6:36-60. https://doi.org/10.1007/s11947-012-0867-9
Ratcliffe M, Panozzo JF (1999). The Application of Near Infrared Spectroscopy to Evaluate Malting Quality. Journal of the Institute of Brewing 105(2):85-88.
Rubinsztain Y, Yariv S, Ioselis P, Aizenshtat Z, Ikan R (1986). Characterization of melanoidins by IR spectroscopy—I. Galactose-glycine melanoidins. Organic Geochemistry 9(3):117-125.
Sá RM de, Palmer GH (2006). Analysis of β-Glucan in Single Grains of Barley and Malt Using NIR-Spectroscopy. Journal of the Institute of Brewing 112(1):9-16.
Schmidt W (2000). Optische Spektroskopie: Eine Einführung, 2nd edn. Wiley-VCH, Weinheim, New York.
Schmidt J, Gergely S, Schönlechner R, Grausgruber H, Tömösközi S, Salgó A, Berghofer E (2009). Comparison of Different Types of NIR Instruments in Ability to Measure β-Glucan Content in Naked Barley. Cereal Chemistry Journal 86(4):398-404.
Sekkal M, Dincq V, Legrand P, Huvenne JP (1995). Investigation of the glycosidic linkages in several oligosaccharides using FT-IR and FT Raman spectroscopies. Journal of Molecular Structure 349:349-352. https://doi.org/10.1016/0022-2860(95)08781-P
Shahidi F, Ambigaipalan P (2015). Phenolics and polyphenolics in foods, beverages and spices: Antioxidant activity and health effects – A review. Journal of Functional Foods 18(B):820-897.
Sharpe FR, Garvey TB, Pyne NS (1992). The Measurement of Beer and Wort Colour - A New Approach. Journal of the Institute of Brewing 98(4):321-324.
Smedley SM (1992). Colour Determination of Beer Using Tristimulus Values. Journal of the Institute of Brewing 98(6):497-504.
Spieleder E (2007). Systematische Untersuchungen von reduzierenden Substanzen und Malz und ihr Einfluss auf den Brauprozess. Dissertation, Technische Universität München.
Streitberger HJ, Dössel KF (eds) (2008). Automotive paints and coatings, 2nd edn. Wiley-VCH-Verl., Weinheim.
Takoi K, Kaneda H, Kikuchi T, Watari J, Takashio M, Yoshimura J, Nishita N, Yamazaki H, Yana J (2003). Application of Compact High-

Performance Electron Spin Resonance for Malt Quality Estimation. Journal of the American Society of Brewing Chemists 61(3):146-151.
Uchida M, Ono M (1996). Improvement for Oxidative Flavor Stability of Beer—Role of OH-Radical in Beer Oxidation. Journal of the American Society of Brewing Chemists 54(4):198-204.
van Boekel MAJS (2006). Formation of flavour compounds in the Maillard reaction. Biotechnology Advances 24(2):230-233.
Wang HY, Qian H, Yao WR (2011). Melanoidins produced by the Maillard reaction: Structure and biological activity. Food Chemistry 128(3):573-584.
Woffenden HM, Ames JM, Chandra S (2001). Relationships between antioxidant activity, color, and flavor compounds of crystal malt extracts. Journal of Agricultural and Food Chemistry 49(11):5524-5530.
Wunderlich S, Wurzbacher M, Back W (2013). Roasting of malt and xanthohumol enrichment in beer. European Food Research and Technology 237:137-148. https://doi.org/10.1007/s00217-013-1970-5
Yahya H, Linforth RST, Cook DJ (2014). Flavour generation during commercial barley and malt roasting operations: a time course study. Food Chemistry 145:378-387.